Some Aspects of Stability and Numerical Dissipation of the Finite-Difference Time-Domain (FDTD) Technique Including Passive and Active Lumped Elements

Werner Thiel and Linda P. B. Katehi, *Fellow, IEEE*

***Abstract*—This paper presents a stability analysis of the extended finite-difference time-domain method including passive and active devices. An explicit, implicit, and semi-implicit incorporation of lumped elements is investigated and the eigenvalues of the resulting discrete system are discussed. With the underlying assumption that the domain is homogeneously loaded with lumped elements, stability criteria are derived on the basis of a resistance, a conductance, and an inductance. Applying a fully implicit method, a parasitic resistance can be observed when reactive devices are included. For an inductance, this numerical dissipation is characterized in detail and an equivalent circuit is given. As an example, the impact on the quality (Q) factor of a cavity loaded with an inductance is shown and compared to the theoretical derivation.**

***Index Terms*—FDTD, integration techniques, lumped elements, numerical dissipation, numerical stability, waveguide resonator.**

I. Introduction

THE finite-difference time-domain (FDTD) technique, first proposed in [1], provides a very flexible numerical method for solving linear and nonlinear electromagnetic problems. Since Maxwell's equations are solved in the time domain on a spatial grid, nonlinear problems can easily be handled in comparison to frequency-domain-based methods.

In nonlinear circuits, active devices are often given by their large-signal equivalent circuit [2] and are included as a lumped element in the FDTD grid using usually two kind of interfaces, i.e., the voltage–source [3] and the current–source [4] approach, respectively. As an alternative to using an equivalent circuit for the nonlinear device, a hybrid technique is proposed in [5]–[7], where the solid-state device is modeled by a finite-difference method and is included as a subsystem in the coarser FDTD grid. In this case, the device is also treated as a lumped element in the FDTD grid and is updated synchronously with the FDTD time step.

However, the interface between the lumped element and FDTD grid, especially the temporal discretization, must be chosen so that a stable discrete system results. In the literature, many different approaches have been reported. With a forward Euler method, as described in [8], the state–space variables of the lumped element can easily be updated in the nonlinear case without applying recursive methods for solving the nonlinear system of equations. This explicit method can also provide a simple interface between the FDTD grid and a circuit simulator [6], which performs the calculation of the circuit of the lumped element. As a disadvantage, this method is only applicable and remains stable for small time steps if the current and voltage of the device are located on different cells in the FDTD grid [8]. For an unconditionally stable method up to the Courant condition of the FDTD scheme, fully implicit [9] and semi-implicit [4], [10] interfaces have been developed and successfully employed to analyze active microwave circuits [9], [11]. However, the stability of the extended FDTD scheme has always been proven based on simulation results and empirical approaches. Therefore, theoretical studies do not exist and stability conditions for the different kinds of temporal discretizations are not available.

In further studies performed on lumped elements, parasitic reactances caused by the FDTD grid, which can seriously affect the behavior of a circuit in the millimeter-wave range, were observed [11]. In the past, these parasitic reactances were characterized and correction procedures were suggested [11]–[13].

The main goal of this paper is to provide stability conditions for explicit and implicit methods and to investigate the existence of numerical dissipation by applying a fully implicit interface. All the considerations in this paper are based on a plane-wave approach for the three-dimensional (3-D) Yee scheme. The derivation of the eigenvalues is based on the assumption that the domain is homogeneously loaded with lumped elements. In Section II, basic principles of an eigenvalue analysis of a difference scheme are described and the eigenvalues for the one-dimensional Yee scheme loaded with an arbitrary linear lumped element are given. This study concentrates on the first-order fully implicit, second-order semi-implicit, and first-order explicit methods and gives a stability analysis for a resistor, a conductor, and an inductor in Sections III–V, respectively. Finally in Section VII, a lossless cavity loaded with an inductance is chosen to demonstrate the existence of a parasitic resistance due to the dissipation effect that the numerical analysis showed.

Manuscript received September 2, 2001. This work was supported by the Common High Performance Computing Software Support/High Performance Computing Modernization Office under Grant DAAD19-00-1-0173.

W. Thiel is with the Department of Electrical Engineering Computer Science, Radiation Laboratory, The University of Michigan at Ann Arbor, Ann Arbor, MI 48109-2122 USA.

L. P. B. Katehi was with the Department of Electrical Engineering Computer Science, Radiation Laboratory, The University of Michigan at Ann Arbor, Ann Arbor, MI 48109-2122 USA. She is now with the Schools of Engineering, Purdue University, West Lafayette, IN 47907 USA.

Publisher Item Identifier 10.1109/TMTT.2002.802330.

II. Extended FDTD Scheme

In this section, the eigenvalues for a homogeneously loaded FDTD grid are derived as a basis for the investigations in the following sections. If a plane wave propagating in z-direction is assumed, the discretized form of one-dimensional Maxwell's equations according to Yee's scheme is

$$\begin{aligned} \epsilon\frac{E_y|_k^{n+1}-E_y|_k^n}{\Delta t} &= \frac{H_x|_{k+1/2}^{n+1/2}-H_x|_{k-1/2}^{n+1/2}}{\Delta z} - \frac{I_{\text{device}}}{\Delta z\Delta x} \\ \mu\frac{H_x|_{k+1/2}^{n+1/2}-H_x|_{k+1/2}^{n-1/2}}{\Delta t}\mu &= \frac{E_y|_{k+1}^n-E_y|_k^n}{\Delta z} \end{aligned} \tag{1}$$

where I_{device} is the current through the lumped element. For an arbitrary nonlinear lumped element, the current through the device can be expressed by

$$I_{\text{device}} = f\left(E_y|_k^{n+1}, E_y|_k^n, E_y|_k^{n-1}, \ldots, E_y|_k^1, E_y|_k^0\right)\frac{\epsilon\Delta x\Delta z}{\Delta t} \tag{2}$$

where $f(\boldsymbol{x})$ represents a nonlinear function in $\boldsymbol{x}$. In the linear case, the current of the device is just a linear combination of the electric fields at previous time steps

$$\begin{aligned} I_{\text{device}} = \Big(&c_{-1}E_y|_k^{n+1} + c_0E_y|_k^n + c_1E_y|_k^{n-1} + \cdots \\ &+ c_{n-1}E_y|_k^1 + c_nE_y|_k^0\Big)\frac{\epsilon\Delta x\Delta z}{\Delta t}. \end{aligned} \tag{3}$$

To perform a stability analysis for the nonlinear case, the nonlinear function $f(\boldsymbol{x})$ can be linearized at each time step. As a matter of fact, the eigenvalues depend on time and global stability analysis becomes more difficult.

If the current of the lumped element is inserted in (1), a multilevel scheme depending on several previous time steps is deduced. The latter can be easily transformed into a two-level scheme by introducing the vector

$$\boldsymbol{u}_k^n = \left(E_y|_k^n, H_x|_{k+1/2}^{n-1/2}, E_y|_k^{n-1}, \ldots, E_y|_k^0\right)^T. \tag{4}$$

For the stability analysis, the finite-difference scheme is expressed in the Fourier domain by the discrete Fourier transform (DFT) [14]

$$\hat{\boldsymbol{u}}^n(\zeta) = \frac{1}{\sqrt{2\pi}}\sum_{k=-\infty}^{\infty} e^{-ik\zeta}\boldsymbol{u}_k \tag{5}$$

with $\zeta \in [-\pi, \pi]$ being a normalized spatial wavenumber. However, this approach is only possible if a domain homogenously loaded with lumped elements is assumed. Finally, the difference scheme can be written in the following form:

$$\mathbf{A}\hat{\boldsymbol{u}}^{n+1} = \mathbf{B}\hat{\boldsymbol{u}}^n. \tag{6}$$

For a stability analysis, the eigenvalues of the matrix $\mathbf{A}^{-1}\mathbf{B}$ have to be investigated. These are the roots of the following polynomial:

$$\begin{aligned} P(\lambda) = (-1)^\eta\Bigg(&\lambda^{\eta+2} - \lambda^{\eta+1}\left(\frac{2+c_{-1}-c_0}{1+c_{-1}} - \frac{4\nu^2\sin^2\frac{\zeta}{2}}{1+c_{-1}}\right) \\ &+\lambda^\eta\frac{1-c_0+c_1}{1+c_{-1}} + \sum_{m=1}^{\eta-1}\lambda^m\frac{c_{\eta-m+1}+c_{\eta-m}}{1+c_{-1}} \\ &-\frac{c_\eta}{1+c_{-1}}\Bigg) \end{aligned} \tag{7}$$

with the Courant number $\nu = \Delta t/(\Delta z\sqrt{\epsilon\mu})$ referred to the unloaded case. The degree of the polynomial $P(\lambda)$ is equal to the number of elements of the vector $\boldsymbol{u}_k^n$ and η corresponds to the additional time levels for the electric field ($E_y|_k^{n-1}$ to $E_y|_k^{n-\eta}$) needed for the time discretization of the lumped element. To get a stable discrete system, the magnitude of all eigenvalues has to be less than one for $\zeta \in [-\pi, \pi]$. In the following sections, the specific values for the constants c_m are taken into account.

III. Resistor

In this section, the stability of a lumped resistor is investigated for different temporal discretization techniques. This problem is related to an FDTD technique including lossy dielectrics. In [15], a stability analysis was performed for the 3-D wave equation.

A. Explicit (Forward Euler)

In the explicit case, the current through the device depends only on the electric field of the previous time step and is given by $I_{\text{device}} = (\Delta y/R)E^n = ((\epsilon\Delta x\Delta z)/(\Delta t))c_0E^n$. Hence, all other coefficients c_m with $m \neq 0$ are zero in (7). The magnitude of the eigenvalues of (7) is less than one if the Courant number ν satisfies the condition

$$\nu \leq \frac{1}{2}\sqrt{4-2c_0}. \tag{8}$$

If this inequality is solved for the time step Δt, the stability condition

$$\Delta t \leq \sqrt{\left(\frac{\Delta y\Delta z\mu}{4R\Delta x}\right)^2 + \Delta z^2\mu\epsilon} - \frac{\Delta y\Delta z\mu}{4R\Delta x} \tag{9}$$

is derived. The latter shows that the time step strongly depends on the resistance R and decreases if the resistance becomes small. On the other hand, the accuracy of that scheme is only first order in time $\mathcal{O}(\Delta t)$.

B. Fully Implicit (Backward Euler)

If a fully implicit method is applied to the resistor, the current $I_{\text{device}} = (\Delta y/R)E^{n+1}$ depends only on the electric field that is currently updated. In this case, only the coefficient c_{-1} is considered in polynomial (7) and all other coefficients are ignored. The evaluation of the eigenvalues leads to the stability condition for the Courant number ν

$$\nu \leq \frac{1}{2}\sqrt{4+2c_{-1}}. \tag{10}$$

Solving again the inequality for the time step Δt

$$\Delta t \leq \sqrt{\left(\frac{\Delta y \Delta z \mu}{4R\Delta x}\right)^2 + \Delta z^2 \mu\epsilon} + \frac{\Delta y \Delta z \mu}{4R\Delta x} \tag{11}$$

it turns out that the time step is less restricted than in the unloaded case. Depending on the value of the resistance, this fully implicit scheme admits a coarser time step, but is only first-order accurate.

C. Semi-Implicit (Leap Frog)

The semi-implicit case is of particular importance because it corresponds to a second-order accurate scheme in time. The scheme is called semi-implicit if at least the coefficient c_{-1} is not zero. First, a current update equation including the current and previous electric field $I_{\text{device}} = (c_{-1}E^{n+1} + c_0 E^n)(\epsilon \Delta x \Delta z)/(\Delta t)$ is considered. A calculation of the eigenvalues according to polynomial (7) gives the following stability condition for the Courant number ν:

$$\nu \leq \frac{1}{2}\sqrt{4 + 2c_{-1} - 2c_0}. \tag{12}$$

This inequality shows that the scheme becomes more stable for $c_{-1} > c_0$ and the time step can be increased beyond the maximum admissible time step of the unloaded case. For $c_{-1} < c_0$, the scheme behaves more explicitly and, as a consequence, the time step is restricted similarly to the explicit case and depends on the resistance R. If $c_{-1} = c_0$, a second-order accurate scheme results, which is stable for a Courant number $\nu \leq 1$.

Some more possibilities for a semi-implicit incorporation of the device are given in Table I. The current

$$I_{\text{device}} = \left(c_{-1}E^{n+1} + c_0 E^n + c_1 E^{n-1} + c_2 E^{n-2}\right)\frac{\epsilon \Delta x \Delta z}{\Delta t} \tag{13}$$

now depends on the electric field up to the time step $n-2$. For all these values of the coefficients c_m listed in Table I, a fixed limit for the Courant number results and does not depend on the resistance. If time steps beyond $n-2$ are used or if the values of the coefficients are changed, the maximum applicable Courant number will be a function of the resistance and, in most cases, an analytic expression for the eigenvalues cannot be derived.

IV. Capacitor

In contrast to the resistor, the stability condition for a capacitor is of interest only for an explicit and implicit temporal discretization because, in this case, the current is the temporal derivative of the electric field and, therefore, directly related to the leap-frog scheme.

A. Explicit

In the explicit case, the current through the capacitor depends on the electric field on the time steps n and $n-1$ and, therefore, the nonzero coefficients according to (3) are

$$c_0 = -c_1 = \frac{C\Delta y}{\epsilon \Delta x \Delta z} \tag{14}$$

TABLE I
Courant Number Limit for Several Semi-Implicit Methods and Accuracy in Time

accuracy	c_0/c_{-1}	c_1/c_{-1}	c_2/c_{-1}	$\nu \leq$
$\mathcal{O}(\Delta t^2)$	1	0	0	1
$\mathcal{O}(\Delta t)$	0	1	0	$1/\sqrt{2}$
$\mathcal{O}(\Delta t)$	0	0	1	$1/2$
$\mathcal{O}(\Delta t)$	1	1	0	$\sqrt{3}/2$
$\mathcal{O}(\Delta t)$	1	1	1	1

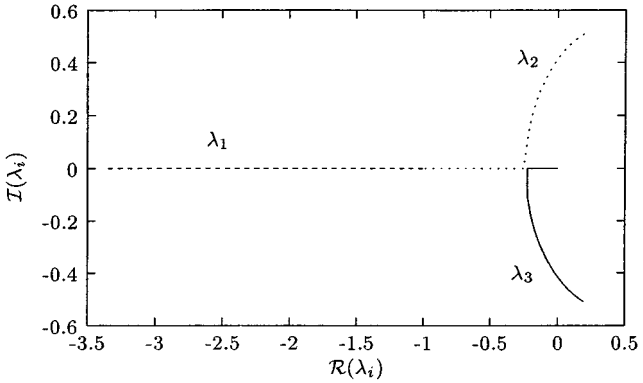

Fig. 1. Eigenvalues in the complex plane associated with the explicit scheme $\nu = 1$.

where C is the capacitance. For the capacitance, an analytic expression for the stability criterion cannot be derived. To this end, the eigenvalues of the discrete system can only be studied for fixed Courant numbers ν. The magnitude of the three eigenvalues is shown in Fig. 1 for the Courant number $\nu = 1$. The system is unstable for all capacitances C because at least one of the eigenvalues has a magnitude larger than one. For a small Courant number $\nu \to 0$, the magnitudes of the eigenvalues converge to $|\lambda_1| = |\lambda_2| = 1$ and $|\lambda_3| = c_0$. As a consequence, the difference scheme is only stable and a time step $\Delta t > 0$ only exists, if the coefficient $c_0 < 1$. That implies that the ratio of the grid capacitance over the capacitance of the lumped element is one at the maximum.

B. Implicit

The implicit inclusion of a capacitor can be regarded as an increase of the grid capacitance by the lumped capacitance because the temporal discretization is identical with the leap-frog scheme and the domain is homogeneously loaded with the capacitors. Inserting the coefficients

$$c_{-1} = -c_0 = \frac{C\Delta y}{\epsilon \Delta x \Delta z} \tag{15}$$

in (7), the following stability criterion is deduced:

$$\nu \leq \sqrt{1 + c_{-1}}. \tag{16}$$

This is exactly the Courant stability criterion for a domain with grid capacitance increased by a factor $1 + c_{-1}$, where c_{-1} represents the ratio of the grid capacitance $\epsilon \Delta x/\Delta y$ over lumped capacitance $C/\Delta z$ per length.

V. Inductor

Problems emerge in the case of a lumped inductor if a stability analysis is based on (7) for the eigenvalues. Due to the time integral of the electric field, an infinite number of coefficients are nonzero and this makes the computation of the eigenvalues nearly impossible. To this end, a state vector I_{device} is introduced to avoid the infinite sum over all electric-field updates. This approach reduces the degree of the polynomial to three.

A. Explicit

The derivative of the device current depends on the electric field at the past time step only and can be formulated in the explicit case as

$$I_{\text{device}}^{n+1} = I_{\text{device}}^{n} + \frac{\Delta y \Delta t}{L} E^{n} \tag{17}$$

where I_{device}^{n+1} corresponds to the device current I_{device} of (1). The eigenvalues of the discrete system yield a stability condition for the Courant number ν

$$\nu \leq \frac{1}{2}\sqrt{4-\eta} \tag{18}$$

with

$$\eta = \frac{(\Delta t^2 \Delta y)}{(L\epsilon \Delta x \Delta z)}. \tag{19}$$

Resolving the inequality for the time step

$$\Delta t \leq \frac{1}{\sqrt{\frac{1}{\Delta z^2 \epsilon \mu} + \frac{\Delta y}{4L\epsilon \Delta x \Delta z}}} \tag{20}$$

it turns out that the time step has to be decreased by an amount that is proportional to the square root of the inductance. With this approach, a nondissipative difference scheme is obtained because the magnitude of all eigenvalues is one

$$|\lambda_{1,2,3}| = 1 \qquad \forall \zeta \in [-\pi, \pi] \tag{21}$$

where Δt satisfies the stability condition.

B. Semi-Implicit

If a temporal average is employed for the electric field, a second-order accurate scheme is obtained. Hence, the current in (1) becomes

$$I_{\text{device}}^{n+1} = I_{\text{device}}^{n} + \left(\frac{\Delta y \Delta t}{L}\right) \frac{E^{n+1} + E^{n}}{2} \tag{22}$$

where $(I_{\text{device}}^{n+1} + I_{\text{device}}^{n})/2$ corresponds to the device current I_{device} of (1). This semi-implicit difference scheme is stable for a Courant number $\nu \leq 1$ independently of the value of the inductance. The magnitude of the eigenvalues are

$$|\lambda_{1,2,3}| = 1 \qquad \forall \zeta \in [-\pi, \pi] \text{ and } \nu \in [0, 1] \tag{23}$$

so that, in this case, a nondissipative difference scheme also results. As a consequence, the scheme remains stable under the stability condition of the unloaded case.

C. Fully Implicit

In the fully implicit case, only the electric field at the current time step $n+1$ is taken into account. Therefore, the current through the inductor has the form

$$I_{\text{device}}^{n+1} = I_{\text{device}}^{n} + \frac{\Delta y \Delta t}{L} E^{n+1}. \tag{24}$$

If the current is specified according to (3), an alternative expression

$$I_{\text{device}} = \frac{\Delta y \Delta t}{L} \sum_{m=0}^{n+1} E^{m} \tag{25}$$

is obtained, which is proposed for an implicit incorporation of the inductance in [10]. An evaluation of the eigenvalues gives the following stability condition for this method

$$\nu \leq \frac{1}{2}\sqrt{4+\eta} \tag{26}$$

where η is defined in (19). This inequality shows that the scheme is stable even for $\nu \geq 1$ depending on the value of the inductance. In contrast to the explicit and semi-implicit method, the magnitude of two of the eigenvalues

$$|\lambda_1| = 1,\ |\lambda_{2,3}| = \frac{1}{1+\eta} \qquad \forall \zeta \in [-\pi, \pi] \tag{27}$$

is less than one, which implies a numerical dissipation of the difference scheme. In Section VII, the effect of numerical dissipation on microwave circuits is discussed in detail for a cavity loaded with an inductance.

VI. Nonlinear Lumped Elements

In this section, the stability analysis described in Section II is applied to nonlinear elements. In case of a nonlinear element, the current of the device can be expressed by

$$I_{\text{device}} = f\left(E_y|_k^{n+1}, E_y|_k^{n}, E_y|_k^{n-1}, \ldots, E_y|_k^{1}, E_y|_k^{0}\right) \cdot \frac{\epsilon \Delta x \Delta z}{\Delta t}. \tag{28}$$

If this equation is linearized by

$$\Delta I_{\text{device}} = \left(c_{-1}\Delta E_y|_k^{n+1} + c_0 \Delta E_y|_k^{n} + c_1 \Delta E_y|_k^{n-1} + \cdots + c_{n-1}\Delta E_y|_k^{1} + c_n \Delta E_y|_k^{0}\right) \frac{\epsilon \Delta x \Delta z}{\Delta t} \tag{29}$$

with

$$c_i = \left.\frac{\partial f}{\partial E_y|_k^{n-i}}\right|_{E_y|_k^{n}} \tag{30}$$

at the operating point and only the differential values are considered, the eigenvalues of the polynomial $P(\lambda)$ provide an estimation of the local stability at this particular time step. Furthermore, the coefficients c_i also depend on space and, therefore, a Fourier transform to eliminate the spatial number k cannot be performed. However, at each single grid point and at every time

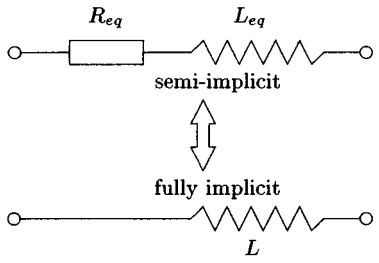

Fig. 2. Equivalent circuit for an inductance included by a fully implicit method.

step, a polynomial can be obtained if partially homogeneous loaded lines are assumed in order to employ the analysis for the linear lumped elements. The eigenvalues yielding the most restrictive stability criterion are taken for an estimation of the global stability.

As an example, a diode with the current voltage characteristic

$$I_{\text{device}} = I_D \left(e^{U/U_T} - 1 \right) \tag{31}$$

is considered. The minimal differential resistance $r_D = (I_D/U_T)e^{U/U_T}$ can be inserted in the stability criteria for the resistance obtained in Section III and leads to a condition for the time step in the explicit, implicit, and semi-implicit cases.

VII. Numerical Dissipation

Although the inductance is a reactive device, the fully implicit incorporation in the FDTD grid leads to eigenvalues with a magnitude less than one. Hence, the electric field will decrease exponentially in time. If a discrete Fourier mode $\boldsymbol{u}_k^n = \hat{\boldsymbol{u}} e^{i\omega n\Delta t + i\beta k\Delta z}$ is inserted in the difference scheme, a complex frequency $\omega = \alpha - ib$ is obtained. Between the magnitude of the eigenvalue and attenuation constant b exists the following relationship:

$$e^{b\Delta t} = |\lambda|. \tag{32}$$

For a large inductance, the attenuation constant b for the fully implicitly included inductor can be approximated by

$$b = -\Delta t \frac{\left(\dfrac{\Delta y}{L\epsilon \Delta x \Delta z} \right)}{\left(1 + \dfrac{\Delta t^2 \Delta y}{L\epsilon \Delta x \Delta z} \right)}. \tag{33}$$

Hence, the attenuation is quasi-proportional to the time step and, therefore, the parasitic dissipation can only be decreased by using small time steps in the FDTD simulation. According to Fig. 2, the dissipative inductor can be replaced by an equivalent circuit consisting of an inductance and a resistance modeled by the semi-implicit scheme. In the equivalent circuit, the inductor is a nondissipative element and only the resistance represents the lossy part. If the eigenvalues of the serial connection of the inductor and resistor are investigated, it turns out that, in comparison to (27), the magnitude of the eigenvalues depends on the wavenumber β. To this end, the resistance is also a function of the wavenumber

$$R_{\text{eq}} = f(L, \Delta t, \beta) \tag{34}$$

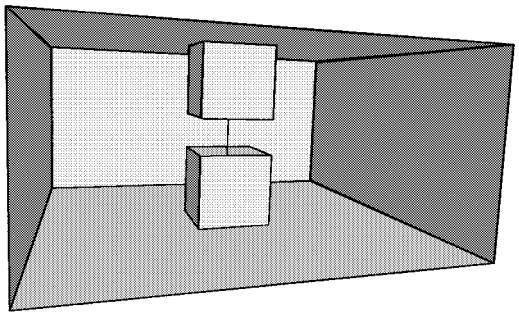

Fig. 3. Cavity in the Ka-band loaded with an inductor.

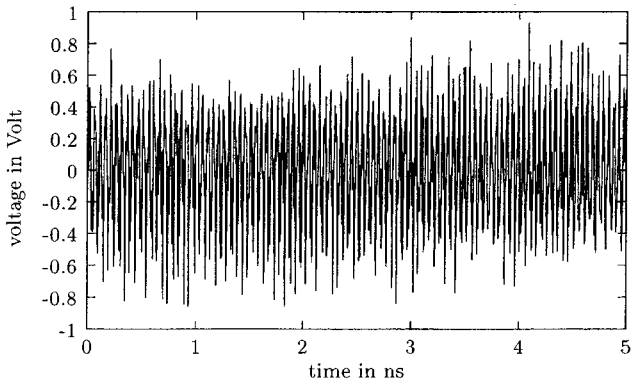

Fig. 4. Voltage across the inductance for the semi-implicit scheme in the time domain.

and the equivalent circuit is only valid for a small-signal analysis.

As a numerical example in the 3-D case, a cavity in the Ka-band loaded with an inductor, as shown in Fig. 3, is analyzed to illustrate the impact of the numerical dissipation on the Q factor. The waveguide resonator is discretized by $10 \times 10 \times 5$ cells and the lumped inductance is placed in the center of the cavity between two perfect electric conducting pads with a size of 2×2 cells. At the boundary surface, the resonator is excited with the TE_{10} mode and a delta function in the time domain to cover a wide frequency band. A time step of 1.2 ps is used for the analysis and the signal is recorded for 38 ns. The Q factor of the loaded cavity is determined by performing a DFT of the time signal. Two resonances in the cavity are considered: The TE_{101} mode at 29.77 GHz and the TE_{201} at 47.07 GHz. Due to the inductive load of 0.8953 nH, the resonance frequencies are shifted and are observed at 32.65 and 51.48 GHz. The electric field across the inductance for the fully implicit and the semi-implicit incorporation is shown in the time domain in Figs. 4 and 5, respectively. As the semi-implicit method is nondissipative, the amplitude of the signal does not decay in time and, hence, a infinite Q factor is achieved. Applying the fully implicit method instead, an exponential attenuation of the signal is visible according to Fig. 5. The spectra of both signals around 51.5 GHz are given in Fig. 6. Whereas the semi-implicit approach leads to an infinitely small bandwidth, the bandwidth for the fully implicit approach is increased by the parasitic resistance and, as consequence, a finite Q factor is obtained. On the other hand, the resonant frequencies of the two inclusion methods are slightly different

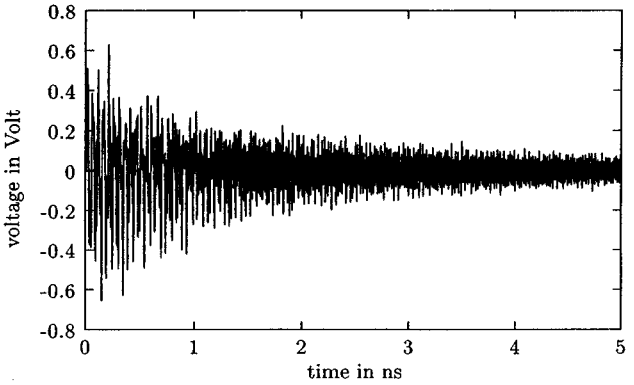

Fig. 5. Voltage across the inductance for the fully implicit scheme in the time domain.

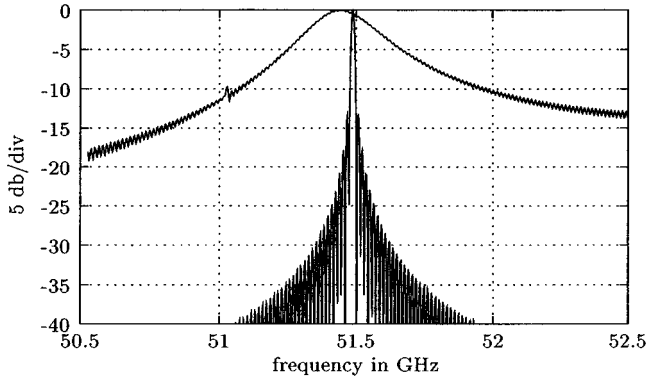

Fig. 6. Spectra around 51.5 GHz for the semi and fully implicit scheme.

TABLE II
CAVITY LOADED WITH A FULLY IMPLICIT INCORPORATED INDUCTANCE. EVALUATION OF PARAMETERS AT TWO RESONANT FREQUENCIES FOR $L = 0.8953$ nH AND $\Delta t = 1.187$ ps (ATTENUATION CONSTANT: $b = \pi f_r/Q$)

f_r (GHz)	Δf (MHz)	Q	b (s^{-1})	R_{eq} (Ω)
32.65	274	118	0.867×10^9	134
51.48	274	188	0.867×10^9	134

because of their different accuracy orders. To this reason, the equivalent inductance in Fig. 2 is, like the equivalent resistance, a function of the time step, inductance, and wavenumber β. In Table II, the attenuation constant b, equivalent resistance $R_{\rm eq}$, and other evaluated parameters of the cavity are listed for the two frequencies. Since the eigenvalues given in (27) are independent of the wavenumber, the attenuation constant b is also independent of the frequency (confirmed in Table II). At both frequencies, the numerical dissipation corresponds to an equivalent resistance of 134 Ω.

In a further simulation, the time step is divided by two and the change in the attenuation constant is compared to the analytic expression (2). As expected, the attenuation constant given in Table III is also divided by two. Table III also shows the attenuation for the case of a double inductance. The attenuation constant decreases and a higher Q factor is achieved. If the complex impedance of the inductor is considered, the resistive part comes in the range of the reactive part of the complex impedance for large time steps and small inductances; e.g., the impedance of the inductor at 51.48 GHz according to Table II is $(j290 + 134)\Omega$.

TABLE III
CAVITY LOADED WITH A FULLY IMPLICIT INCORPORATED INDUCTANCE. PARAMTERS FOR DOUBLED INDUCTANCE AND HALVED TIME STEP

f_r (GHz)	Δf (MHz)	Q	b (s^{-1})	R_{eq} (Ω)
$\Delta t/2$				
51.24	134	383	0.420×10^9	57
$2 \times L$				
51.03	80	638	0.251×10^9	109

VIII. CONCLUSION

In this paper, a stability analysis of the extended FDTD method including lumped elements has been presented. All calculations are based on a plane-wave approach and on the assumption that the whole domain is homogeneously loaded. Stability conditions for the implicit and explicit methods were derived for a resistor, an inductor, and a capacitor. An eigenvalue analysis of the fully implicitly incorporated inductance showed the existence of a parasitic resistance. The impact on the electromagnetic behavior of microwave circuits has been demonstrated and validated on the basis of a cavity in the Ka-band. To this end, it turns out that the fully implicit approach, corresponding to the forward Euler applied to the state variables of the lumped element, is not only first-order accurate, but also dissipative. Finally, the trapezoidal integration method has proven to be a suitable semi-implicit second-order scheme for the incorporation of a lumped element into the FDTD.

REFERENCES

[1] K. S. Yee, "Numerical solution of initial boundary value problems involving Maxwell's equation in isotropic media," *IEEE Trans. Antennas Propagat.*, vol. AP-14, pp. 302–307, May 1966.

[2] W. Thiel and W. Menzel, "FDTD analysis of a quasiplanar MM-wave frequency doubler," in *IEEE MTT-S Int. Microwave Symp. Dig.*, 1998, pp. 881–884.

[3] C.-N. Kuo, R.-B. Wu, B. Houshmand, and T. Itoh, "Modeling of microwave active devices using the FDTD analysis based on the voltage–source approach," *IEEE Microwave Guided Wave Lett.*, vol. 6, pp. 199–201, May 1996.

[4] W. Sui, D. A. Christensen, and C. H. Durney, "Extending the two-dimensional FDTD method to hybrid electromagnetic systems with active and passive lumped elements," *IEEE Trans. Microwave Theory Tech.*, vol. 40, pp. 724–730, Apr. 1992.

[5] W. Thiel, M. Birk, W. Menzel, and P. Abele, "A global finite difference time domain analysis of silicon nonlinear transmission line," in *IEEE MTT-S Int. Microwave Symp. Dig.*, 2000, pp. 371–374.

[6] R. Witzig, W. Schuster, P. Regli, and W. Fichtner, "Global modeling of microwave applications by combining the FDTD method and a general semiconductor device and circuit simulator," *IEEE Trans. Microwave Theory Tech.*, vol. 47, pp. 919–928, June 1999.

[7] P. Ciampolini, L. Roselli, and G. Stopponi, "Integrated FDTD and solid-state device simulation," *IEEE Microwave Guided Wave Lett.*, vol. 6, pp. 419–421, Nov. 1996.

[8] J. Mix, J. Dixon, Z. Popović, and M. Piket-May, "Incorporating nonlinear lumped elements in FDTD: The equivalent source method," *Int. J. Numer. Modeling*, vol. 12, pp. 157–170, 1999.

[9] C.-M. Malgorzata and W. K. Gwarek, "Implicit incorporation of nonlinear elements for unconditionally stable FDTD analysis at coarse time-steps," in *IEEE MTT-S Int. Microwave Symp. Dig.*, 1996, pp. 1381–1384.

[10] M. Piket-May, A. Taflove, and J. Baron, "FDTD modeling of digital signal propagation in 3-D circuits with passive and active loads," *IEEE Trans. Microwave Theory Tech.*, vol. 42, pp. 1514–1523, Aug. 1994.

[11] W. Thiel and W. Menzel, "Full-wave design and optimization of MM-wave diode based circuits in finline technique," *IEEE Trans. Microwave Theory Tech.*, vol. 47, pp. 2460–2466, Dec. 1999.
[12] V. S. Reddy and R. Garg, "An improved extended FDTD formulation for active microwave circuits," *IEEE Trans. Microwave Theory Tech.*, vol. 47, pp. 1603–1608, Sept. 1999.
[13] R. Gillard, S. Dauguet, and J. Citerne, "Correction procedures for numerical parasitic elements associated with lumped elements in global electromagnetic simulators," *IEEE Trans. Microwave Theory Tech.*, vol. 46, pp. 1298–1306, Sept. 1998.
[14] J. W. Thomas, *Numerical Partial Differential Equations, Finite Difference Methods*. New York: Springer-Verlag, 1995.
[15] J. A. Perada, O. Garcia, A. Vegas, and A. Prieto, "Numerical dispersion and stability analysis of the FDTD technique in lossy dielectrics," *IEEE Microwave Guided Wave Lett.*, vol. 8, pp. 245–247, July 1998.

Werner Thiel was born in Altoetting, Germany, in 1970. He received the Dipl.-Ing. and Dr.-Ing. degrees from the University of Ulm, Ulm, Germany, in 1995 and 2000, respectively.

From 1995 to 2001, he was a Research Assistant with the Microwave Techniques Department, University of Ulm, where he was involved with the development of FDTD software and the design and optimization of nonlinear components in the millimeter wave applying the FDTD method. Since April, 2001 he has been a Research Fellow with the Department of Electrical Engineering Computer Science, Radiation Laboratory, The University of Michigan at Ann Arbor. His research activities and interests are computational electromagnetics with emphasis on the FDTD technique, with applications to microelectromechanical structures (MEMS) and large-scale communication problems.

Linda P. B. Katehi (S'81–M'84–SM'89–F'95) received the B.S.E.E. degree from the National Technical University of Athens, Athens, Greece, in 1977, and the M.S.E.E. and Ph.D. degrees from the University of California at Los Angeles, in 1981 and 1984, respectively.

In September 1984, she joined the faculty of the Electrical Engineering and Computer Science Department, The University of Michigan at Ann Arbor, as an Assistant Professor, and then became an Associate Professor in 1989 and Professor in 1994. She has served in many administrative positions, including Director of Graduate Programs, College of Engineering (1995–1996), Elected Member of the College Executive Committee (1996–1998), Associate Dean For Graduate Education (1998–1999), and Associate Dean for Academic Affairs (since September 1999). She is currently the Dean of the Schools of Engineering, Purdue University, West Lafayette, IN. She has authored or co-authored 410 papers published in refereed journals and symposia proceedings and she holds four U.S. patents. She has also generated 20 Ph.D. students.

Dr. Katehi is a member of the IEEE Antennas and Propagation Society (IEEE AP-S), the IEEE Microwave Theory and Techniques Society (IEEE MTT-S), Sigma Xi, Hybrid Microelectronics, and URSI Commission D. She was a member of the IEEE AP-S AdCom (1992–1995). She was an associate editor for the IEEE TRANSACTIONS ON MICROWAVE THEORY AND TECHNIQUES and the IEEE TRANSACTIONS ON ANTENNAS AND PROPAGATION. She was the recipient of the 1984 IEEE AP-S W. P. King (Best Paper Award for a Young Engineer), the 1985 IEEE AP-S S. A. Schelkunoff Award (Best Paper Award), the 1987 National Science Foundation Presidential Young Investigator Award, the 1987 URSI Booker Award, the 1994 Humboldt Research Award, the 1994 University of Michigan Faculty Recognition Award, the 1996 IEEE MTT-S Microwave Prize, the 1997 International Microelectronics and Packaging Society (IMAPS) Best Paper Award, and the 2000 IEEE Third Millennium Medal.